멤브레인(Membrane Journal)
Vol. 33 No. 1 February 2023, 13-22

Print ISSN: 1226-0088
Online ISSN: 2288-7253
DOI: https://doi.org/10.14579/MEMBRANE_JOURNAL.2023.33.1.13

압전 특성의 보호층을 통한 리튬 금속 전지의 전기화학적 특성 개선

박 대 웅*·신 원 호**·손 희 상*,†

*광운대학교 화학공학과, **광운대학교 전자재료공학과
(2022년 12월 21일 접수, 2022년 12월 29일 수정, 2022년 12월 29일 채택)

The Enhanced Electrochemical Performance of Lithium Metal Batteries through the Piezoelectric Protective Layer

Dae Ung Park*, Weon Ho Shin, and Hiesang Sohn*,†**

*Department of Chemical Engineering, Kwangwoon University, Seoul 01897, Republic of Korea
**Department of Electronic Material Engineering, Kwangwoon University, Seoul 01897, Republic of Korea
(Received December 21, 2022, Revised December 29, 2022, Accepted December 29, 2022)

요 약: 리튬 금속 기반 전극의 높은 용량에도 불구하고, 제어가 어려운 덴드라이트 성장은 낮은 쿨롱 효율, 안전 문제를 야기해, 리튬금속 배터리의 상용화를 제한한다. 본 연구에서는 압전 복합체인 $BaTiO_3$/PVDF (BTO@PVDF) 기반 보호층을 리튬금속에 코팅, 덴드라이트에 의한 부피팽창으로 발생한 변형을 분극을 이용하여, 리튬 금속 전극의 안정성 및 성능을 향상하고자 한다. 이를 통해, 균일한 리튬이온의 증착이 가능해졌으며, BTO@PVDF 전극은 100 사이클 동안 약 98.1% 이상의 쿨롱 효율을 나타내었다. 또한, CV를 통해 향상된 리튬이온의 확산계수(D_{Li+}) 증가를 보였으며, 본 연구에서 제시된 전략은 리튬 금속 전극의 성능 향상에 새로운 길을 나타내준다.

Abstract: Despite high capacity of lithium metal anode, its uncontrollable dendrite growth results in the poor electrochemical (EC) performance (low Coulomb efficiency and limited cycle stability) and unsafe operation. In this study, we demonstrated a lithium metal anode protected with $BaTiO_3$/PVDF based piezoelectric layer to enhance its EC performance by utilizing the locally polarized lithium metal after volume expansions. As-formed lithium metal electrode deposited with BTO@PVDF layer exhibited an enhanced Coulombic efficiency (> 98% for 100 cycles) and facilitated lithium ion diffusions (lithium diffusion coefficient: D_{Li+}), revealing the effectiveness of piezoelectric layer deposited lithium metal electrode approach.

Keywords: *β-phase PVDF, $BaTiO_3$, piezoelectric effect, lithium metal, anode*

1. Introduction

The surging energy consumption brought the demand for lithium ion batteries with high energy density and elongated life[1-6]. As of the successful commercialization of Sony's lithium-ion batteries (LIBs), the graphite has been employed as anode material because of its stable electrochemical reaction of lithium ions, low self-discharge, and high structural stability during long charge/discharge. Despite the advantages of graphite based anode, it has a limitations to enhance the energy density of the battery due to its low specific capacity (372 mAh/g)[7,8].

To boost up the EC performance of LIBs, there have been many development to enhance the EC performance (capacity and energy density) of the anode of lithium ion battery[9-20]. Among them, the lithium

†Corresponding author(e-mail: sonisang@hanmail.net; http://orcid.org/0000-0002-4164-9397)

metal anode have been highlighted due to its low reduction potential[−3.04 V (vs. SHE)], high theoretical specific capacity (3,860 mAh/g) and potential application towards next-generation batteries such as lithium-sulfur and lithium-air batteries[21-24]. Despite many advantages of lithium metal battery, the practical application is undermined because of unsatisfactory EC performance and unsafeness at elongated charge/discharges[25]. Such problems can be attributed to the uneven lithium deposition by non-uniform distribution of the lithium nucleus and subsequent uneven electrodeposition of Li, and lithium dendrites formation [25,26]. In addition, the uneven lithium surface can further generate fine lithium particles (dead lithium) separated from the current collector and induce to form porous Lithium metal with high surface area, leading to promoted side reactions, rapidly consumed liquid electrolyte and increased cell impedance[27,28]. As-suggested drawback of lithium metal electrode convection always exists in the mass transfer process on the surface of the Lithium anode, which inevitably causes non-uniform Li-ion flux, resulting in non-uniform Lithium precipitation after long-term cycling[29].

In this context, there have been many studies on the improvement of the lithium negative electrode through various approaches including i) restructuring of electrode[30-34] and ii) introduction of functional protective layer on the lithium electrode to accommodate the uniform lithium ion distribution, reduced volume change and stabilized interface between electrode/electrolyte[35-43]. As-proposed approaches could successfully suppress the growth of Lithium dendrite and improve the Coulombic efficiency (CE).

Considering the importance of controlled lithium ion flux, it is crucial to make a dendrite-free lithium metal for the successful commercialization of LMB[30]. In this respect, we prepared a piezoelectric nanocomposite protective layer of $BaTiO_3$ @poly(vinylidene fluoride (BTO@PVDF) to achieve a uniform lithium deposition and improved EC performance.

In this study, we demonstrate a piezoelectric nanocomposite of BTO@PVDF as protective layer for the uniform lithium ion control to utilize the compressive stress generated from volume expansion of lithium during the deposition/desorption of lithium. Note that, A piezoelectric field formed by the corresponding stress can promote ion transport and make the non-uniform flux of lithium ions, leading to enhanced EC performance of the lithium metal anode[44]. As-formed piezoelectricity of BTO@PVDF was confirmed by its crystal structure and output voltage generated under a pressure. In addition, the electrochemical characteristics of the lithium metal anode protected with BTO@PVDF layer was analyzed by their Cyclic voltammogram (CV) behavior at various scan rates and coulombic efficiency, peak currents and overpotentials at elongated cycles.

2. Experimental

2.1. Materials

BTO nanopowder (< 100 nm, 99% purity, Sigma-Aldrich), polyvinylidene fluoride (PVDF, M. W. 534,000, Sigma-Aldrich) and N,N-Dimethylformamide (DMF, anhydrous 99.8%, Alfa Aesar) were used without further purification for the synthesis of BTO@PVDF composite.

2.2. Fabrication of piezoelectric protective layer on lithium metal electrode

2.2.1. Preparation of precursor solution for BTO@PVDF

A 5 mL solution of 35 wt% barium titanate (BTO) dispersed in N-N Dimethylformamide (DMF, anhydrous 99.8%) and a 50 mL DMF solution of 15 wt% Polyvinylidene fluoride (PVDF) were stirred for 8 hours at 35°C. Then, as-formed solutions were mixed and stirred at 700 RPM for 3 hours, followed by air bubble removal under vacuum for 30 min.

2.2.2. Fabrication of BTO@PVDF composite thin film and its electrode

As-prepared BTO@PVDF precursor was further coated to be fabricated as composite thin film as protective layer. Specifically, the copper (Cu) foil pre-

treated with 1M HCl was coated with BTO@PVDF precursor through two-step spin coating (step 1: 30 s and 300 rpm, step 2: 60 s and 2000 rpm). As-coated composite thin film of BTO@PVDF was further dried in a vacuum oven at 60°C for 12 hours followed by additional drying at 100°C for 2 hours.

2.3. Material Characterization

The surface morphology of the piezoelectric composite film of BTO@PVDF and its electrode was characterized by SEM (FE-SEM, HITACH, S-4800). The crystal structure of the BTO@PVDF film for the phase transition analysis was characterized at a 2θ range of 10-80° with X-ray diffractometer (MiniFlex 600) using CuK α (=0.154059 nm) as radiation source. The piezoelectricity of the BTO@PVDF composite film was analyzed by generated currents and voltages with an oscilloscope (Keithley DSOX2004A).

2.4. Electrochemical characterization

The electrochemical performance of the lithium metal anode treated with piezoelectric composite layer was analyzed with a CR-2032 coin type half-cell. Lithium foil was used as a counter electrode while an electrode coated with a BTO@PVDF thin film was used as a working electrode. An electrolyte was prepared and used with 1M lithium bis(trifluoromethanesulfonyl) imide (LITFSI) lithium salt and 2 wt% of $LiNO_3$ additive dissolved in mixed solvent of 1,3-dioxolane (DOL) and 1,2-dimethoxyethane (DME) (1:1 v/v). Celgard 2400 was used as the separator.

In the half-cell test, the coulombic efficiency and overpotential were measured using a battery tester (WBCS3000, Wonatech). Both the counter and reference electrodes were Lithium metals. Coulombic efficiency (CE) and overpotential of the untreated and BTO@PVDF treated lithium electrodes were compared at a voltage range of 0.02 to 1.2 V and at a current density of 1mA/cm^2 under a plating and stripping capacity of 1 mAh/cm^2.

3. Results and Discussion

3.1. Piezoelectric BTO@PVDF composite thin film as protective layer

As displayed in the Scheme 1, the piezoelectric composite of BTO@PVDF as protective layer was prepared by combining the advantage of organic matrix (PVDF) and inorganic filler (BTO). Briefly, the disturbed electron clouds of BTO@PVDF composite un-

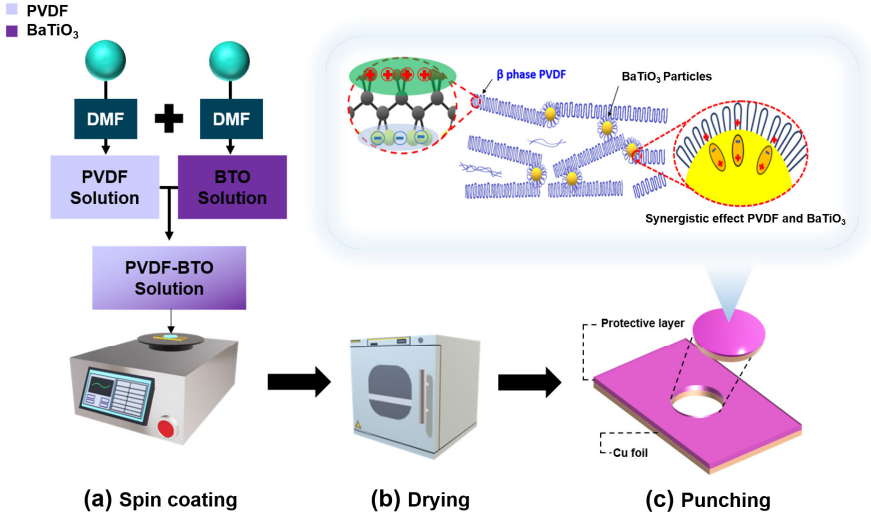

Scheme 1. Preparation of BTO@PVDF protective layer and its piezoelectric effects (a) Spin coating BTO@PVDF on Cu, (b) Drying in vacuum oven, (c) Punching the coated Anode.

der pressure induces to form a piezoelectric potential by the charge flowing through the PVDF for the restoration of the charge equilibrium. The interplay of BTO particles and charges generated by PVDF stacks further accumulate the piezoelectric potential by the accumulation effect, leading to an enhanced piezoelectric effect by β-phase PVDF and BTO particles[45].

We demonstrated aforementioned piezoelectric effect by endowing β-PVDF with a role of piezoelectric polymer to chemically/flexibly bond on lithium metal surface through an adaptive adhesion and granting a perovskite $BaTiO_3$ ceramic with high piezoelectric constant and mechanical strength[46-53]. In order to make β-PVDF film, the BTO@PVDF film annealed at 100°C exhibit the enhanced β-phased PVDF by the quenching process. As-formed PVDF films containing both polar and non-polar phases depend on the molecular structure of fluorine (F). Reportedly, the stretching and annealing of PVDF thin films increase the β-phase content of PVDF[55-57]. Specifically, α-PVDF film is non-polar as F atoms take the trans-gauche conformation alternating with their antiparallel dipole moments. However, β-PVDF films polarized by F atoms exhibit parallel dipole moments and all-trans conformations[46,54].

3.2. Material characterization

The morphology of the BTO@PVDF composite thin film as protective layer was analyzed by electronic imaging with scanning electron microscopy (SEM). (Fig. 1) Fig. 1a displays a the cross-sectional image of BTO@PVDF composite thin film (ca. 29.4 μm) uniformly deposited on Cu current collector. Fig. 1b displays the plane image of BTO@PVDF composite thin film taken with SEM, suggesting homogeneous dispersion of BTO particles in the PVDF matrix[58].

As shown in Fig. 2, the maximum output voltage was obtained under pressure (100 kPa) application of the BTO@PVDF electrode at 1 V, confirming the piezoelectricity of the protective layer. In the EC cell, as-applied pressure on the BTO@PVDF electrode on lithium electrode can be estimated as 100 kPa by calculating overpotential due generated by mechanical blocking[59].

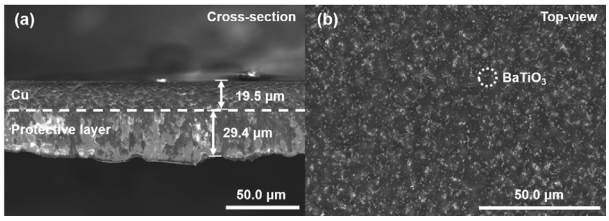

Fig. 1. SEM image of BTO@PVDF/Li electrode (a) Cross-section view (b) Top-view.

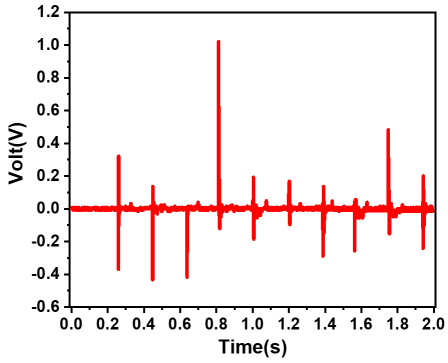

Fig. 2. Output voltage of BTO@PVDF thin film under constant pressure 100 kPa.

3.3. Electrochemical analysis

As shown in the Fig. 3a, Coulombic efficiency (CE) for the lithium metal anodes with and without BTO@PVDF protective layer were compared using half-cell based on repeatedly deposited/desorbed lithium on Cu foil as the working electrode. Note that, the BTO@PVDF protective layer exhibited maintained CE (>95%) up to 130 cycles, whereas CE of the bare Cu decreased with cycles (< 90% at 60 cycles). Fig.s 3b and c exhibit the voltage profiles of bare Cu and BTO@PVDF electrodes at various cycles. The bare Cu electrode exhibits a distinctive overpotential at a reduced capacity after 80 cycles. What is worse, the overvoltage increased from 29 mV (10th cycle) to 50.8 mV (80th cycle) with cycles. In contrast, the lithium electrode with the BTO@PVDF protective layer exhibits the maintained overpotential at a constant capacity even after the long cycles, confirming the stabilized cell by protective layer.

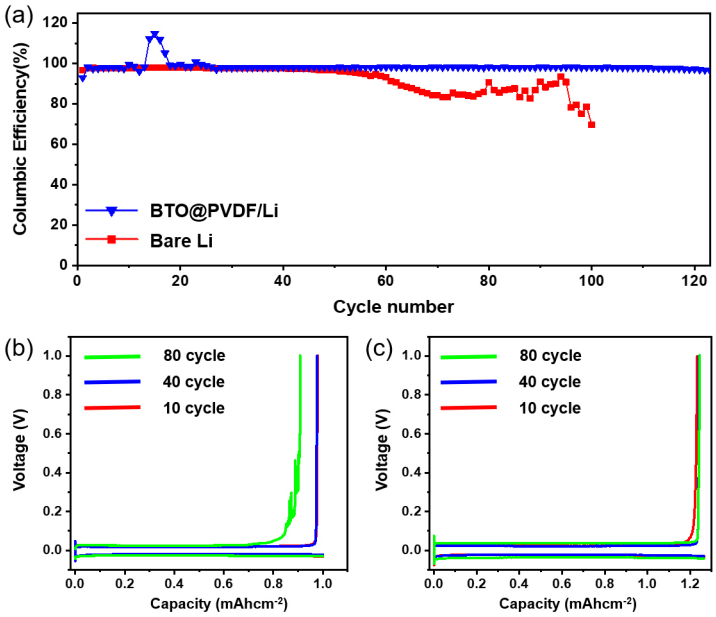

Fig. 3. Electrochemical analysis of bare Li and BTO@PVDF/Li electrodes (a) Coulombic efficiency; Voltage profiles of the 10th, 40th, and 80th cycles (b) bare Cu, (c) BTO@PVDF treated electrodes.

The irreversible Lithium loss of bare Cu based electrode is attributable to a chemical reaction of lithium with the electrolyte to form SEI or electrically isolated Lithium particles. In this regards, the BTO@PVDF protective layer play an important role to reduce the contact between Lithium and the electrolyte, allowing the uniform Lithium deposition and suppressed chemical reactions and an alleviated formation of dead Lithium particles.

Fig. 4 display the electronic images of lithium electrode prepared with and without BTO@PVDF protective layer. As shown in Fig. 4a, bare lithium electrode shows non-uniform and porous lithium metal layer (*ca.* 97.6 μm) after repeated electrodeposition at 1 mA/cm^2 for 50 hours (Fig. 4a) and lithium dendrites (Fig. 4b). In contrast, the lithium electrode coated with BTO@PVDF layer displays relatively small lithium metal deposition (*ca.* 58.5 μm) underneath the protective layer without noticeable deformation (Fig. 4c). As shown in the plane view of lithium electrode coated with protective layer (Fig. 4d), much more smooth electrode surface indicates the suppressed lithium dendrites formation by alleviated direct contact of the

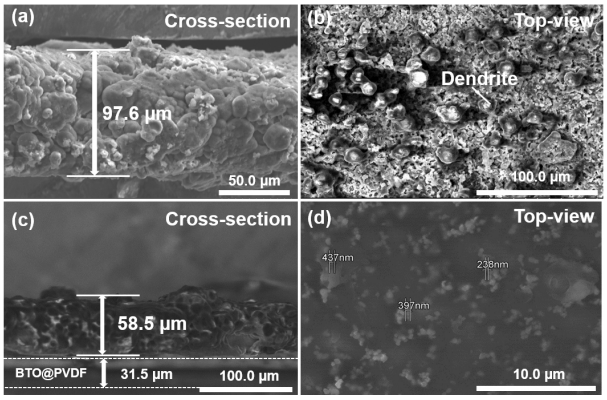

Fig. 4. SEM images of (a,b) bare Li and BTO@PVDF/Li (c,d) electrodeposited with lithium after cycling at 1 mA/cm^2 for 50 hours.

electrolyte with electrode, leading to reduced electrolyte consumption and interfacial resistance[60].

The piezoelectric nanocomposite thin film as a protective layer plays an important role to enhance the EC performance of the lithium metal electrode. As more Li^+ is deposited on the localized electrode under the application of low current density (0.025~0.5 mA/cm^2), so relatively large lithium nuclei are formed with inhomogeneous Li^+ flux because of retarded mobility of

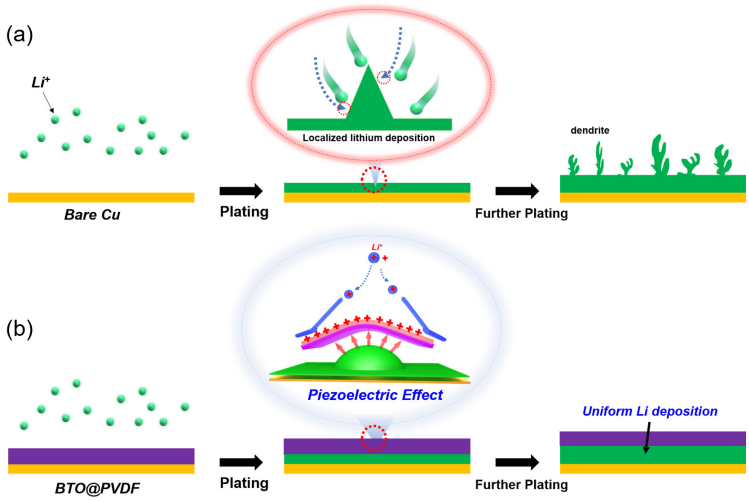

Scheme 2. Schematic illustration of piezoelectric protective layer effect on lithium metal anode.

Li^+[61]. As shown in Scheme 2a, Such non-uniform distribution of lithium nucleus on the electrode surface subsequently lead to a uneven electrodeposition of lithium and its dendrites, resulting in the precipitation of lithium on anode surface after long-term cycling[40]. However, as shown in Scheme 2b, the BTO@PVDF composite as protective layer induces homogeneous transport of lithium ions[44] while the inductive stress (compressive stress by lithium dendrites) generates the piezopotential of the protective layer by piezoelectricity[44]. Such uniform deposition of lithium ion from vertical to lateral, leading to effective elimination of lithium[62].

4. Conclusion

In this report, we demonstrated the enhanced EC performance of lithium metal anode by applying a piezoelectric organic/inorganic nanocomposite of BTO@PVDF as protective layer to endow a local polarizability with lithium anode. As-deposited BTO@PVDF on lithium metal electrode exhibited an enhanced Coulombic efficiency (> 98% for 100 cycles at 1 mA/cm^2 and stable voltage gradient at elongated cycles (~80 cycles) and facilitated lithium ion diffusions (D_{Li+}:2.4 × 10^{-18}cm^2/s), suggesting the effective function of piezoelectric protective layer on lithium metal electrode. allows uniform lithium ions and was improved due to stabilization of the lithium metal cathode.

Considering the importance of a uniform lithium ion flux and a dendrite-free lithium metal anode, we believe the application of the piezoelectric BTO@PVDF composite film as protective layer on the lithium metal anode leads to successful commercialization of lithium metal battery with high capacity and stability.

Acknowledgement

The present research has been conducted by the Research Grant of Kwangwoon University in 2021. This research was supported by the Nano-Material Technology Development Program through the National Research Foundation of Korea (NRF), funded by the Ministry of Science, ICT and Future Planning (2009-0082580). It was also supported by an NRF grant funded by the Korean government (MSIT) (No. NRF-2020R1F1A1065536) and Korea Electric Power Corporation (KEPCO) (No. 2022-0909).

Reference

1. F. Dai, R. Yi, H. Yang, Y. Zhao, L. Luo, M. L. Gordin, H. Sohn, S. Chen, C. Wang, S. Zhang, and D. Wang, “Minimized volume expansion in hi-

erarchical porous silicon upon lithiation", *ACS Appl. Mater. Interfaces*, **11**, 13257 (2019).
2. H. Sohn, D. H. Kim, R. Yi, D. Tang, S. E. Lee, Y. S. Jung, and D. Wang, "Semimicro-size agglomerate structured silicon-carbon composite as an anode material for high performance lithium-ion batteries", *J. Power Sources*, **334**, 128 (2016).
3. D. Y. Oh, Y. E. Choi, Y. G. Lee, J. N. Park, H. Sohn, and Y. S. Jung, "All-solid lithium-ion batteries with TiS_2 nanosheet and sulfide solid electrolytes", *J. Mater. Chem. A*, **4**, 10329 (2016).
4. Q. Xiao, H. Sohn, Z. Chen, D. Toso, M. Mecklenburg, Z. H. Zhou, E. Poirier, A. Dailly, H. Wang, Z. Wu, M. Cai, and Y. Lu, "Mesoporous metal and metal alloy particles synthesized by aerosol-assisted confined growth of nanocrystals", *Angew. Chem. Int. Ed.*, **51**, 10546 (2012).
5. G. Eshetu, H. Zhang, X. Judez, H. Adenusi, M. Armand, S. Passerini, and E. Figgemeier, "Production of high-energy Li-ion batteries comprising silicon-containing anodes and insertion-type cathodes", *Nature Commun.*, **12**, 5459 (2021).
6. Y. Ding, Z. Cano, A. Yu, J. Lu, and Z. Chen, "Automotive Li-Ion batteries: current status and future perspectives", *Electrochem. Energ.*, **2**, 1 (2019).
7. S. Kim, "Recent developments in anode materials for Li secondary batteries", *J. Kor. Electrochem. Soc.*, **3**, 211 (2008).
8. S. Sivakkumar, J. Nerkar, and A. Pandolfo, "Rate capability of graphite materials as negative electrodes in lithium-ion capacitors", *Electrochim. Acta*, **55**, 3330 (2010).
9. P. Guo, H. Song, and X. Chen, "Electrochemical performance of graphene nanosheets as anode material for lithium-ion batteries", *Electrochem. Commun.*, **11**, 1320 (2009).
10. J. Lim, J. Won, M. Kim, D. Jung, M. Kim, S. Koo, J. Oh, H. Jeong, H. Sohn, W. Shin, and C. Park, "Synthesis of flower-like manganese oxide for accelerated surface redox reactions on nitrogen-rich graphene of fast charge transport for sustainable aqueous energy storage", *J. Mater. Chem. A*, **10**, 7668 (2022).
11. Y. Jeong, J. Park, S. Lee, S. H. Oh, W. J. Kim, Y. J. Ji, G. Y. Park, D. Seok, W. Shin, J. Oh, T. Lee, C. Park, A. Seubsaic, and H. Sohn, "Iron oxide-carbon nanocomposites modified by organic ligands: Novel pore structure design of anode materials for lithium-ion batteries", *J. Elec. Anal. Chem.*, **904**, 115905 (2022).
12. K. Hwang, N. Kim, Y. Jeong, H. Sohn, and S. Yoon, "Controlled nanostructure of a graphene nanosheet-TiO_2 composite fabricated via mediation of organic ligands for high-performance Li storage applications", *Int. J. Energy Res.*, **45**, 16189 (2021).
13. D. Seok, W. Shin, S. Kang, and H. Sohn, "Piezoelectric composite of $BaTiO_3$-coated SnO_2 microsphere: Li-ion battery anode with enhanced electrochemical performance based on accelerated Li^+ mobility", *J. Alloys Comp.*, **870**, 159267 (2021).
14. M. Kim, D. Ko, J. Kim, E. Cho, D. Yang, C. Kwak, and H. Sohn, "Silver nanowires network film with enhanced crystallinity toward mechano-electrically sustainable flexible-electrode", *Adv. Mater. Inter.*, **6**, 2000838 (2020).
15. H. Sohn, W. Shin, D. Seok, T. Lee, C. Park, J. Oh, S. Kim, and A. Seubsai, "Novel hybrid conductor of irregularly patterned graphene mesh and silver nanowire networks", *Micromachines*, **11**, 578 (2020).
16. D. Seok, Y. Kim, and H. Sohn, "Synthesis of Fe_3O_4/porous carbon composite for efficient Cu^{2+} ions removal", *Membr. J.*, **29**, 308 (2019).
17. D. Seok, Y. Jeong, K. Han, D. Yoon, and H. Sohn, "Recent progress of electrochemical energy devices: Metal oxide–carbon nanocomposites as materials for next-generation chemical storage for renewable energy", *Sustainability*, **11**, 3694 (2019).
18. H. Sohn, Q. Xiao, A. Seubsai, Y. Ye, J. Lee, H. Han, S. Park, G. Chen, and Y. Lu, "Thermally robust porous bimetallic (Ni_xPt_{1-x}) alloy particles within carbon framework: High-performance catalysts for hydrogenation reaction and oxygen reduction reaction", *ACS Appl. Mater. Interfaces*, **11**,

21435 (2019).
19. K. Hwang, H. Sohn, and S. Yoon, "Mesostructured niobium-doped titanium oxide-carbon (Nb-TiO_2-C) composite as an anode for high-performance lithium-ion batteries", *J. Power Sources*, **378**, 225 (2018).
20. H. Sohn, S. Kim, W. Shin, J. Lee, K. Moon, H. Lee, D. Yun, I. Han, C. Kwak, and S. Hwang, "Novel flexible transparent conductive films with enhanced chemical and electro-mechanical sustainability: TiO_2 nanosheet-Ag nanowire hybrid", *ACS Appl. Mater. Interfaces*, **10**, 2688 (2018).
21. K. Kisu, S. Kim, T. Shinohara, K. Zhao, A. Züttel, and S. Orimo, "Monocarborane cluster as a stable fluorine-free calcium battery electrolyte", *Sci. Rep.*, **11**, 7563 (2021).
22. L. Liu, Y. Yin, J. Li, N. Li, X. Zeng, H. Ye, Y. Guo, and L. Wan, "Free-standing hollow carbon fibers as high-capacity containers for stable lithium metal anodes", *Joule*, **1**, 563 (2017).
23. P. G. Bruce, S. A. Freunberger, L. Hardwick, and J. Tarascon, "Li-O_2 and Li-S batteries with high energy storage", *Nature Mater.*, **11**, 19 (2012).
24. X. Liang, Q. Pang, I. Kochetkov, M. Sempere, H. Huang, X. Sun, and L. Nazar, "A facile surface chemistry route to a stabilized lithium metal anode", *Nature Energy*, **2**, 17119 (2017).
25. N. Xu, L. Li, Y. He, Y. Tong, and Y. Lu, "Understanding the molecular mechanism of lithium deposition for practical high-energy lithium-metal batteries", *J. Mater. Chem. A*, **8**, 6229 (2020).
26. A. Pei, G. Zheng, F. Shi, Y. Li, and Y. Cui, "Nanoscale nucleation and growth of electrodeposited lithium metal", *Nano Lett.*, **17**, 1132 (2017).
27. C. Fang, J. Li, M. Zhang, Y. Zhang, F. Yang, Z. Lee, M. Lee, J. Alvarado, M. Schroeder, Y. Yang, B. Lu, N. Williams, M. Ceja, L. Yang, M. Cai, J. Gu, K. Xu, X. Wang, and Y. Meng, "Quantifying inactive lithium in lithium metal batteries", *Nature*, **572**, 511 (2019).
28. H. Zhou, S. Yu, H. Liu, and P. Liu, "Protective coatings for lithium metal anodes: recent progress and future perspectives", *J. Power Sources*, **450**, 227632 (2020).
29. X. Cheng, C. Zhao, Y. Yao, H. Liu, and Q. Zhang, "Recent advances in energy chemistry between solid-state electrolyte and safe lithium-metal anodes", *Chem.*, **5**, 74 (2019).
30. D. Lin, Y. Liu, Z. Liang, H. Lee, W. Sun, J. Wang, H. Yan, J. Xie, and Y. Cui, "Layered reduced graphene oxide with nanoscale interlayer gaps as a stable host for lithium metal anodes", *Nature Nanotechnol.*, **11**, 626 (2016).
31. S. Liu, A. Wang, Q. Li, J. Wu, K. Chio, J. Huang, and J. Luo, "Crumpled graphene balls stabilized dendrite-free lithium metal anodes", *Joule*, **2**, 184 (2018).
32. R. Zhang, X. Cheng, C. Zhao, H. Peng, J. Shi,, J. Huang, J. Wang, F. Wei, and Q. Zhang, "Conductive nanostructured scaffolds render low local current density to inhibit lithium dendrite growth", *Adv. Mater.*, **28**, 2155 (2016).
33. C. Yang, Y. Yin, S. Zhang, N. Li, and Y. G. Guo, "Accommodating lithium into 3D current collectors with a submicron skeleton towards long-life lithium metal anodes", *Nature Commun.*, **6**, 8058 (2015).
34. Q. Li, S. Zhu, and Y. Lu, "3D porous Cu current collector/Li-metal composite anode for stable lithium-metal batteries", *Adv. Mater.*, **27**, 1606422 (2017).
35. W. Li, H. Yao, K. Yan, G. Zheng, Z. Liang, Y. Chiang, and Y. Cui, "The synergetic effect of lithium polysulfide and lithium nitrate to prevent lithium dendrite growth", *Nature Commun.*, **6**, 7436 (2015).
36. X. Cheng, R. Zhang, C. Zhao, and Q. Zhang, "Toward safe lithium metal anode in rechargeable batteries: A review", *Chem. Rev.*, **117**, 10403 (2017).
37. Y. Gao, Z. Yan, J. Gray, X. He, D. Wang, T. Chen, Q. Huang, Y. Li, H. Wang, S. Kim, T. Mallouk, and D. Wang, "Polymer–inorganic solid–

electrolyte interphase for stable lithium metal batteries under lean electrolyte conditions", *Nature Mater.*, **18**, 384 (2019).
38. D. Lin, Y. Liu, and Y. Cui, "Reviving the lithium metal anode for high-energy batteries", *Nature Nanotechnol.*, **12**, 194 (2017).
39. X. Zhang, X. Cheng, and Q. Zhang, "Advances in interfaces between Li metal anode and electrolyte", *Adv. Mater. Interfaces.*, **5**, 1701097 (2018).
40. X. Cheng, R. Zhang, C. Zhao, and Q. Zhang, "Toward safe lithium metal anode in rechargeable batteries: A review", *Chem. Rev.*, **117**, 10403 (2018).
41. S. Lee, S. Choi, J. Hyun, D. Kim, Y. Park, J. Yu, S. Jeon, J. Park, W. Shin, and H. Sohn, "Nanostructured PVdF-HFP/TiO_2 composite as protective layer on lithium metal battery anode with enhanced electrochemical performance", *Membr. J.*, **31**, 417 (2021).
42. S. Lee, D. Seok, Y. Jeong, and H. Sohn, "Surface modification of Li metal electrode with PDMS/GO composite thin film: controlled growth of Li layer and improved performance of lithium metal battery (LMB)", *Membr. J.*, **30**, 38 (2020).
43. Y. Jeong, D. Seok, S. Lee, W. Shin, and H. Sohn, "Polymer/inorganic nanohybrid membrane on lithium metal electrode: Effective control of surficial growth of lithium layer and its improved electrochemical performance", *Membr. J.*, **30**, 30 (2020).
44. J. Xiang, Z. Cheng, Y. Zhao, B. Zhang, L. Yuan, Y. Shen, Z. Guo, Y. Zhang, J. Jiang, and Y. Huang, "A lithium-ion pump based on piezoelectric effect for improved rechargeability of lithium metal anode", *Adv. Sci.*, **6**, 1901120 (2019).
45. L. Lu, W. Ding, J. Liu, and B. Yang, "Flexible PVDF based piezoelectric nanogenerators", *Nano Energy*, **78**, 105251 (2020).
46. Y. Yang, W. Guo, Y. Zhang, Y. Ding, X. Wang, and Z. Wang, "Piezotronic effect on the output voltage of P3HT/ZnO micro/nanowire heterojunction solar cells", *Nano Lett.*, **11**, 4812 (2011).
47. S. Shin, Y. Kim, M. Lee, J. Jung, and J. Nah, "Hemispherically aggregated $BaTiO_3$ nanoparticle composite thin film for high-performance flexible piezoelectric nanogenerator", *ACS Nano*, **8**, 2766 (2014).
48. Y. Zhao, Q. Liao, G. Zhang, Z. Zhang, Q. Liang, X. Liao, and Y. Zhang, "Highoutput piezoelectric nanocomposite generators composed of oriented $BaTiO_3$ NPs@PVDF", *Nano Energy*, **11**, 719 (2015).
49. J. Fu, Y. Hou, X,. Gao, M. Zheng, and M. Zhu, "Highly durable piezoelectric energy harvester based on a PVDF flexible nanocomposite filled with oriented $BaTi_2O_5$ nanorods with high power density", *Nano Energy*, **52**, 391 (2018).
50. Mokhtari, F. Spinks, G. Fay, C. Cheng, Z. Raad, R. Xi, and J. Foroughi, "Wearable electronic textiles from nanostructured piezoelectric fibers", *Adv. Mater. Technol.*, **5**, 1900900 (2020).
51. W. Li-zhu, Z. Chang-song, W. Chu, and W. Ru-peng, "The preparation of PVDF-BTO composite film and the influence of polarization intensity on the piezoelectric properties of composite film", *J. Appl. Phys.*, **1948**, 012191 (2021).
52. X. Guan, B. Xu, and J. Gong, "Hierarchically architected polydopamine modified $BaTiO_3$@P(VDF-TrFE) nanocomposite fiber mats for flexible piezoelectric nanogenerators and self-powered sensors", *Nano Energy*, **70**, 104516 (2020).
53. Y. Wu, G. Wang, Z. Jiao, Y. Fan, P. Peng, and X. Dong, "High electrostrictive properties and energy storage performances with excellent thermal stability in Nb-doped $Bi_{0.5}Na_{0.5}TiO_3$-based ceramics", *RSC Adv.*, **9**, 21355 (2019).
54. Martins P, Lopes, and A. Lanceros-Mendez, "Electroactive phases of poly(vinylidene fluoride): determination, processing and applications", *Prog. Polym. Sci.*, **39**, 683 (2014).
55. V. Cardoso, F. Catarino, S. Serrado Nunes, J. Rebouta, L. Rocha, J. Lanceros-Méndez, and S. Minas, "Lab-on-a-chip with beta-poly(vinylidene fluoride) based acoustic microagitation", *IEEE. Trans. Biomed. Eng.*, **57**, 1184 (2010).

56. V. Cardoso, G. Minas, C. Costa, C. Tavares, and S. Lanceros-Mendez, "Micro and nanofilms of poly(vinylidene fluoride) with controlled thickness, morphology and electroactive crystalline phase for sensor and actuator applications", *Smart Mater. Struct.*, **20**, 087002 (2011).
57. P. Sajkiewicz, A. Wasiak. and Z. Goclowski, "Phase transitions during stretching of poly(vinylidene fluoride)", *Eur. Polym. J.*, **35**, 423 (1999).
58. I. Wan, X. Zhang, Z. Liu, J. Zhang, Z. Li, Z. Lin Wang, and L. Li, "Noninvasive manipulation of cell adhesion for cell harvesting with piezoelectric composite film", *Appl. Mater. Today*, **25**, 101218 (2021).
59. T. Gao, C. Rainey, and W. Lu, "Piezoelectric mechanism and a compliant film to effectively suppress dendrite growth", *ACS Appl. Mater. Interfaces*, **12**, 51448 (2020)
60. X. Gao, Y. Zhou, D. Han, J. Zhou, D. Zhou, W. Tang, and J. Goodenough, "Thermodynamic understanding of Li-dendrite formation", *Joule*, **4**, 1864 (2020).
61. A. Pei, G. Zheng, F. Shi, Y. Li, and Y. Cui, "Nanoscale nucleation and growth of electrodeposited lithium metal", *Nano Lett.*, **17**, 1132 (2017).
62. S. Xia, Y. Zhao, J. Yan, J. Yu, and B. Ding, "Dynamic regulation of lithium dendrite growth with electromechanical coupling effect of soft $BaTiO_3$ ceramic nanofiber films", *ACS Nano*, **15**, 3161 (2021).